SCIENCE FOR CONSERVATION 318

Physical marine environment of the Kermadec Islands region

Phil Sutton, Stephen Chiswell, Richard Gorman, Sean Kennan and Graham Rickard

newzealand.govt.nz

Department of Conservation
Te Papa Atawhai

Cover: Aerial view of Base Camp with Meyer Islands in the background, Raoul Island, Kermadec Islands, 2009. *Photo: DOC.*

Science for Conservation is a scientific monograph series presenting research funded by New Zealand Department of Conservation (DOC). Manuscripts are internally and externally peer-reviewed; resulting publications are considered part of the formal international scientific literature.

This report is available from the departmental website in pdf form. Titles are listed in our catalogue on the website, refer www.doc.govt.nz under *Publications*, then *Science & technical*.

ISSN 1177–9241 (web PDF)
ISBN 978–0–478–14962–3 (web PDF)

This report was prepared for publication by the Publishing Team; editing by Sue Hallas and layout by Elspeth Hoskin and Lynette Clelland. Publication was approved by the Deputy Director-General, Science and Technical Group, Department of Conservation, Wellington, New Zealand.

Published by Publishing Team, Department of Conservation, PO Box 10420, The Terrace, Wellington 6143, New Zealand.

In the interest of forest conservation, we support paperless electronic publishing.

CONTENTS

Physical marine environment of the Kermadec Islands region

Phil Sutton[1], Stephen Chiswell[1], Richard Gorman[2], Sean Kennan[1,3] and Graham Rickard[1]

[1] NIWA, Private Bag 14-901, Kilbirnie, Wellington 6241, New Zealand
Email: p.sutton@niwa.co.nz.

[2] NIWA, PO Box 11115, Hillcrest, Hamilton 3251, New Zealand

[3] Current address: Virginia, USA

Abstract

The ocean surrounding the Kermadec Islands is unique in the greater New Zealand region. Situated c. 1000 km northeast of New Zealand near the centre of the South Pacific Subtropical Gyre, the area is largely isolated and includes the largest marine reserve in New Zealand. This study seeks to describe the physical environment of the ocean surrounding the Islands, including surface and deep currents, temperature and salinity stratification, surface chlorophyll and temperature, and the wave climate. Information is drawn from remote satellite measurements, direct measurements from surface and profiling floats, and models. The region has generally weak current flows, with variability in the flow fields dominating the mean flows. There is also strong variability in the stratification, likely as a result of internal tides. Simulations of larval transports indicate possible exchange times between the islands of the Kermadec Group in the order of 3–10 days, but that exchange between mainland New Zealand and the Islands would take 30–50 days. The wave environment is dominated by higher waves in winter and a propensity to swell from the south. Knowledge of the physical marine environment will assist interpretation of studies of organisms in the region and inform discussions of the relative connectivity between the Kermadec Islands and mainland New Zealand.

Keywords: Kermadec Islands, salinity, temperature, chlorophyll, connectivity, waves

1. Introduction

The Kermadec Islands (see www.doc.govt.nz/kermadecmap for a map of the region) are situated in a very interesting marine environment. The islands are part of a chain of seamounts that run along the Kermadec Ridge, extending north-northeast from the Bay of Plenty (Fig. 1). Just to the east of the ridge is the Kermadec Trench, which is exceptionally deep (>10 km). To the west of the ridge lies another ridge system—the Colville Ridge. This complex bathymetry is a result of successive subduction zones formed as the Pacific Plate is driven under the Australian Plate. The region is also oceanographically very interesting. The Kermadec Ridge forms the western boundary of the deep South Pacific Ocean, and therefore has a deep western boundary current flowing north along its eastern flank. This deep current occurs below 2000 m depth and is the South Pacific component of the global thermohaline circulation (THC), making it an important part of the global climate system. Because of its global significance, this flow has been the subject of several studies (e.g. Warren et al. 1994; Moore & Wilkin 1998; Whitworth et al. 1999).

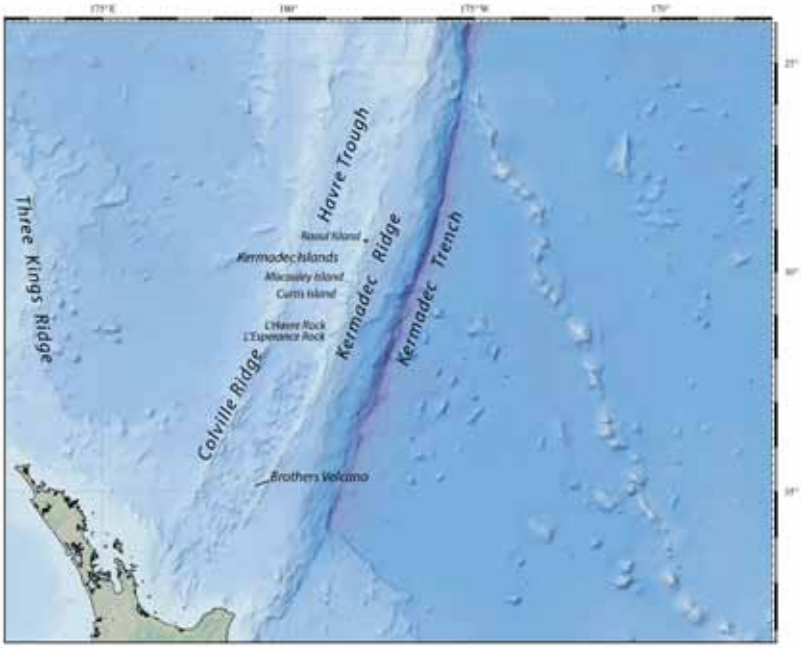

Figure 1. Kermadec Islands in detail.

Nearer the surface, the oceanography is dominated by the South Pacific Subtropical Gyre (Fig. 2), an anticlockwise circulation of subtropical water driven by large-scale winds. Because the study area is in the middle of the subtropical gyre, there are no strong surface fronts or water mass boundaries in the vicinity. This lack of long-term features should not be taken to mean that the area is quiescent; in fact, conditions are quite variable, with the variability being greater than the mean for many of the parameters investigated.

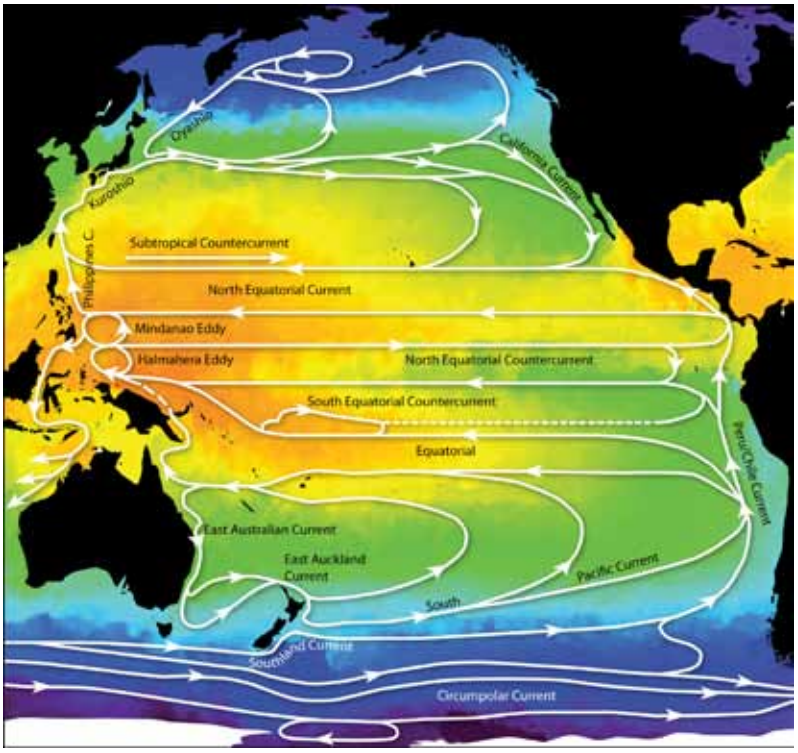

Figure 2. Surface ocean flows in the Pacific Ocean.

Some of the variability in the area is the result of internal tides. These are tides in the ocean interior which are generated by surface tides moving stratified water across sloping topography (in this case the local seamounts and ridge systems). Chiswell & Moore (1999) studied internal tides in the Kermadec Trench using data from moored current meters. They postulate that internal tides generated along the Kermadec Ridge could make a significant contribution to the global

tidal energy dissipation budget. There have been other observations of internal tides in the wider area (Sharples et al. 2001; Stevens et al. 2005), including observations of large internal tides in the upper ocean near the Three Kings Ridge system to the west (Fig. 1).

There is also variability in the flow and property fields resulting from the interaction of larger-scale flows with the extreme bathymetry. This is manifested on occasions by cool sea surface temperatures (SSTs) around islands and over seamounts, presumably resulting from enhanced mixing and/or upwelling. There are almost no data time series collected in proximity to the seamounts and islands. There is, however, a study of the Brothers Volcano, situated south of the study region (Fig. 1) but in a similar environment (Lavelle et al. 2008). There, tidal flows dominated weaker geostrophic upper ocean flows and the near-bed flows were uncorrelated with the surface flows. In addition, Lavelle et al. (2008) found that temperature varied significantly between years.

This report, commissioned by the Department of Conservation (DOC) describes the physical marine environment for an area surrounding the Kermadec Islands, bounded by the coordinates 28°–32°S and 179.4°–177.2°W. The following aspects are addressed:

- Details of the ocean circulation relevant to connectivity between the islands of the archipelago, and between the archipelago and other parts of the southwest Pacific (including the New Zealand mainland).
- The primary productivity within the study area.
- Water column characteristics (temperature and salinity), including temporal, latitudinal and depth-related variation.
- The wave climate (including the orbital velocity at the seabed).

In addition, the possible effects of climate change on these characteristics are discussed.

2. Methods

2.1 Circulation and connectivity

The best estimates of the mean surface currents in the region are from the trajectories traced by Global Drifter Program (GDP) drifters (www.aoml.noaa.gov/phod/dac/gdp.html)(viewed 22 January 2010). These drifters consist of a surface buoy and a drogue (parachute-shaped device) at 15 m depth, meaning that the drifters move with the water at 15-m depth rather than being blown by surface winds. The drifters report latitude and longitude via satellite. Figure 3 shows the trajectories of all of the drifters that have passed through the study region between 1979 and 2007. The drifter trajectories can be used to calculate mean velocities by averaging all of the velocity data in latitude/longitude bins. In this analysis, 1° lat/lon bins were used as a compromise between resolution and statistical robustness. Once the means were calculated, variability—as standard deviation of the eddy speed—was calculated using $\sqrt{(u-\bar{u})^2+(v-\bar{v})^2}$, where u and v are the eastward and northward velocity components, respectively, and the overbar denotes the mean.

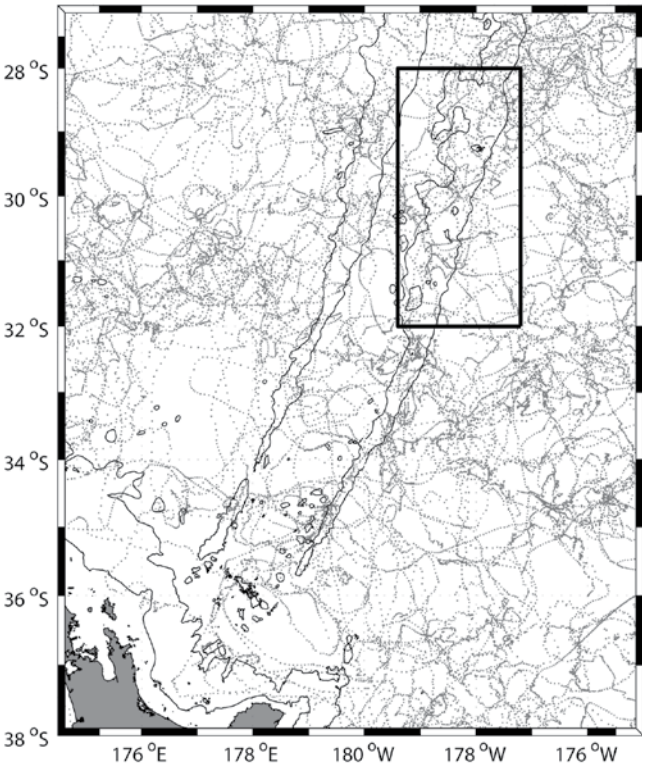

Figure 3. Trajectories of GDP drifters that passed through the Kermadec Islands region 1979–2007. The study region is depicted by the box.

A similar analysis was done using trajectories from Argo floats. Argo floats typically cycle as follows: the float starts at the surface before descending to a parking depth of around 1000 m, where it drifts for 9 days. It then descends further to around 2000 m before ascending, making measurements (typically temperature and salinity) on its way up. Once on the surface, the float transmits the profile data and its location via satellite before repeating the process. Estimating the flow at the parking depth is possible from the consecutive surface locations. Argo floats were first deployed in numbers around New Zealand in 2002, with the global array reaching useful density in 2004.

In order to study connectivity, it is necessary to estimate the time-varying currents. This was done using AVISO products of sea-surface how anomaly field (www.aviso.oceanobs.com/) (viewed 25 January 2010). The flow anomaly field is then combined with the temporal mean current field (estimated from the GDP drifters) to provide estimates of the time-varying current.

Particle (e.g. neutrally-buoyant, passive larvae) trajectories were then simulated from the estimated current fields by numerically seeding the ocean with 'larvae' at specified locations and using standard particle-following Lagrangian techniques. However, it is known that trajectories computed from AVISO currents show less dispersion than expected because interpolation of the satellite-derived currents onto a uniform time and space grid results in a loss of relatively high-frequency variability (Chiswell & Rickard 2008). To compensate for this lack of dispersion, a random-walk diffusion term was added to the larval displacement modelling at each time step.

Similar methods are often used to parameterise sub-grid scale diffusion (for examples, see Olson 2007). The zonal displacement at time $t + \Delta t$ is:

$$x_{t+\Delta t} = L(x_t, u_{t,t+\Delta t}) + \sqrt{2K^+ \Delta t}\,\Re_{0,1}$$

where L is a 4th-order Runge-Kutta Lagrangian integrator, $K+$ is the added eddy diffusivity, and $\Re_{0,1}$ is a random number drawn from a Gaussian distribution having mean = 0 and standard deviation = 1. Eddy diffusivity, $K+$, was set at 1000 m^2/s based on other work done in the New Zealand region (e.g. Chiswell et al. 2007).

Source locations of numerical larvae were chosen to be the islands and where water depths are less than 250 m to provide five source locations along the Kermadec Ridge. A further 12 locations were approximately evenly spaced along the North Island (Tables 1 & 2).

The model was run by seeding 100 larvae at each location every 25 days from 1 January 1993 until November 2007. Thus, there were a total of 109 runs and a total of 10 900 larval releases at each site.

Data from the simulated locations were then compiled to estimate how far larvae were likely to have dispersed 1, 2, 5, 10, 20, 30 and 50 days after release. For example, to estimate the dispersion of larvae 5 days after hatching, positions of all simulated larvae at 5 days after release were compiled in one figure.

TABLE 1. VIRTUAL LARVAE SOURCE LOCATIONS ALONG KERMADEC RIDGE.

LATITUDE	LONGITUDE
-29.251	182.015
-30.226	181.620
-30.578	181.480
-31.319	181.146
-32.411	180.853

TABLE 2. VIRTUAL LARVAE SOURCE LOCATIONS ALONG THE NORTHEAST COAST, NEW ZEALAND.

LATITUDE	LONGITUDE
-38.184	178.445
-37.505	178.357
-37.499	177.922
-37.443	177.095
-37.606	176.577
-36.986	176.098
-36.367	175.781
-35.936	175.173
-35.431	174.711
-34.964	174.046
-34.717	173.409
-34.329	173.005

2.2 Productivity

Satellite-based measurements of ocean colour are the only productivity data covering the region of interest. Monthly chlorophyll and SST data were analysed for the region 28°–32°S, 180°–177°W. Chlorophyll data were derived from ocean colour observations from the SeaWifs mission over the period 1997–2007. SST data are from satellite AVHRR radiometers for 1986–2007 (Reynolds & Smith 1994). For both chlorophyll and SST, the overall means were calculated and the annual cycles investigated.

2.3 Water column characteristics

The data available for studying variability through the water column are temperature and salinity data from Argo profiles.

There are a total of 229 profiles, most of which extend to 2000 m. Because the Argo floats park at a depth of 1000 m, there are not many profiles in water depths shallower than this.

2.4 Wave climate

Two separate wave hindcasts (where past forcings are entered into a model and the output can be compared with known results) were used in this study. Wave analyses involve spectral analysis, where the wave is interpreted as a sum of contributions with different frequencies or harmonics. For spatial distributions of wave statistics, wave model outputs were taken from the NIWA-WAM forecast system (Gorman 2005), running on a grid of longitudes 105°E–220°E (140°W) at 1.25° resolution and latitudes 78°S–0° at 1.00° resolution. Outputs at 3-hourly intervals (apart from some gaps) since February 1997 include summary wave statistics (significant wave height, mean and peak period, mean and peak direction, etc.) over the whole model domain, and full directional spectra at cells near the New Zealand coast.

Hindcast characteristics were then interpolated to finer spatial resolution (0.125° resolution in longitude and 0.10° resolution in latitude) using a 'downwave' method that interpolates wave spectra separately for each propagation direction, and takes account of wave propagation being blocked by land at sub-grid scales. Note, however, that none of the Kermadec Islands were resolved in this interpolation, so the expected 'shadowing' effects of the islands were not accounted for. Also, refraction over the seabed was not taken into account in the computations of the wave spectra.

At each time step, mean-square bed orbital velocities were derived from the spatially-interpolated wave spectra, and mean water depth (from Smith & Sandwell 1997) on the interpolated grid was taken into account.

To provide more details on temporal variability, the NOAA/NCEP Wavewatch III hindcast dataset (Tolman 1999; Tolman et al. 2002) has been used. This provides global hindcasts and forecasts of wave conditions at a resolution of 1.25° for longitude and 1.0° for latitude. Input winds are taken from NCEP's operational Numerical Weather Prediction models. Predictions of wave height, period, direction and associated waves spectral parameters are available every hour. The dataset covers the period 1 February 1997 – 1 July 2008 (providing c. 11.5 years of data). We used outputs at a point (178.75°W, 30°S) near the centre of the study region.

3. Results

3.1 Circulation and connectivity

The mean surface current speed in the study region was weak and dominated by eddies (Fig. 3). In the study area, the mean currents were eastward, with speeds of c. 2–3 cm/s. There is some evidence of speed increase along the ridge. In the same region, the root mean square (rms) eddy speeds were typically 20–40 cm/s. The results from the Argo trajectories indicate that the current speeds at 1000 m depth were typically less than 10 cm/s and tended to be aligned with the bathymetry (Fig. 4).

Figure 5 shows simulated larval dispersion from Raoul Island and the locations along the northeast New Zealand coast 1, 2, 5, 10, 20, 30 and 50 days after release. Results for dispersion from the other islands were similar in behaviour. The simulations showed that, because of the weak mean flow and strong eddy variability, larval exchange can occur in all directions from all islands. Obviously, dispersion of real larvae would critically depend on the life cycle of the organism as well as the oceanography.

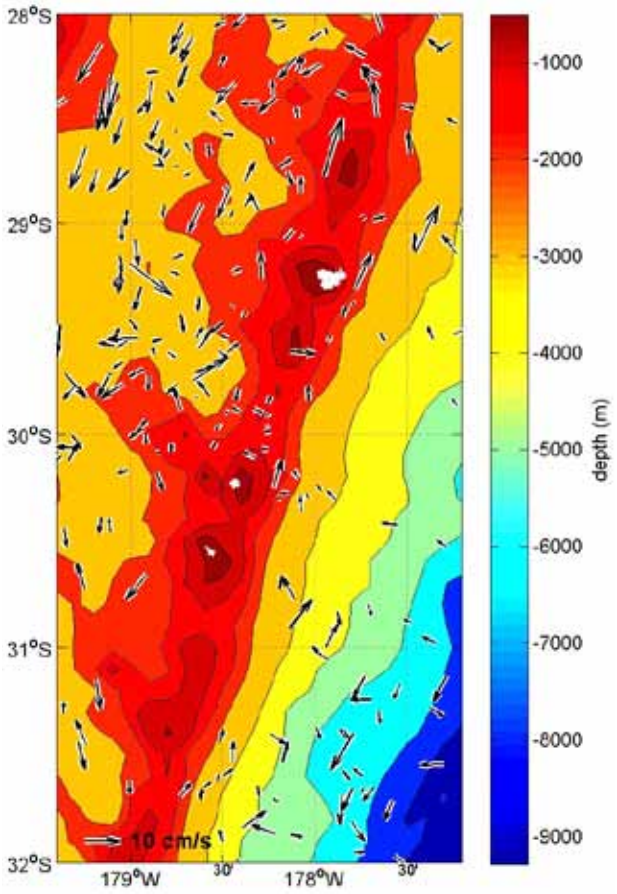

Figure 4. Trajectories of Argo floats, at approximately 1000 m depth, that passed through the region from 2002–3/2010.

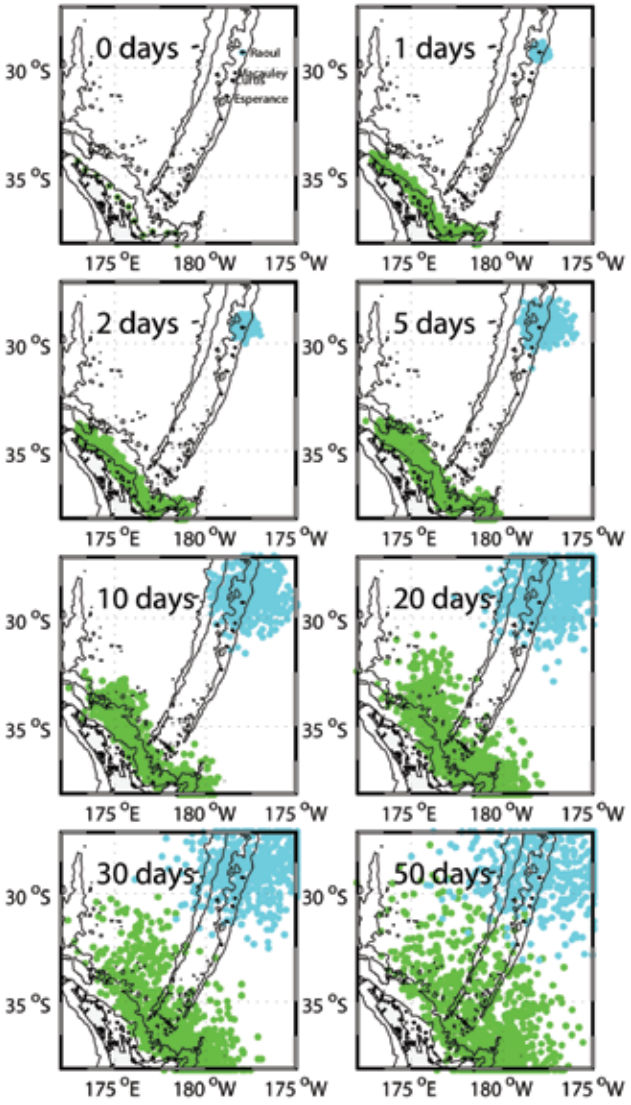

Figure 5. Larval release locations: Raoul Island (blue) and along the northeast coast of New Zealand (green). Dispersion from 1, 2, 5, 10, 20, 30, and 50 days after release.

The estimated minimum larval transport times are:

- From Raoul:
  To Macauley/Curtis: c. 5 days.
  To L'Esperance: c. 10 days.
  To New Zealand mainland: > 50 days.
- From Macauley/Curtis:
  To Raoul: 3–5 days.
  To L'Esperance: c. 5 days.
  To New Zealand mainland: > 50 days.
- From to L'Esperance:
  To Macauley/Curtis: c. 1 day.
  To Raoul: c. 10 days.
  To New Zealand: > 20 days.
- From New Zealand to any of the Kermadec Islands: c. 30 days.

3.2 Productivity and sea surface temperature

The overall patterns of chlorophyll and SST were latitudinal, with cooler, more chlorophyll-rich water to the south, and warmer, chlorophyll-poorer waters to the north (Figs. 6a and 7a). Along the Kermadec Ridge, for a given latitude, surface waters were, on average, cooler and more chlorophyll-rich than those away from the ridge.

The SST data showed a very regular annual cycle, ranging from a minimum of 17°C in August/September to nearly 25°C in February (the mean range was 18°–23.7°C) (Fig. 6b). For any given month, the range in SST was about 2°C.

The chlorophyll data also showed a clear seasonal cycle, but not as sinusoidal as that of SST, with an early spring bloom (Fig. 7b). In addition, while the chlorophyll peaked, on average, in August, the peak sometimes occurred as early as July and as late as September. The total annual range was from c. 0.06 mg/m^3 to more than 0.25 mg/m^3. During summer to early autumn, low values remained (below about 0.1 mg/m^3).

3.3 Water column characteristics

The temperature and salinity profiles from the Argo data (Fig. 8) show quite strong variability (Fig. 9). The seasonal cycle in this area should be limited to the upper 100–200 m (Sutton & Roemmich 2001). There is a systematic change in water properties between the southeastern and northwestern sides of The Kermadec Ridge, with the profiles from the southeast indicating cooler and fresher water at a given depth compared with northwest of the ridge.

3.4 Wave climate

Figure 10 shows the significant wave height averaged over the NIWA-WAM hindcast period, using both the whole record and data from individual calendar months over multiple years. The wave energy flux vector was also averaged over the corresponding times, giving an indication of the average wave propagation directions. Note that this does not mean that waves from the indicated direction occur more often than from other directions: for example, an equal mix of northerly and easterly waves will result in a mean energy flux from the northeast, due to the vector averaging, while an equal mix of northerly and southerly conditions will give zero mean flux.

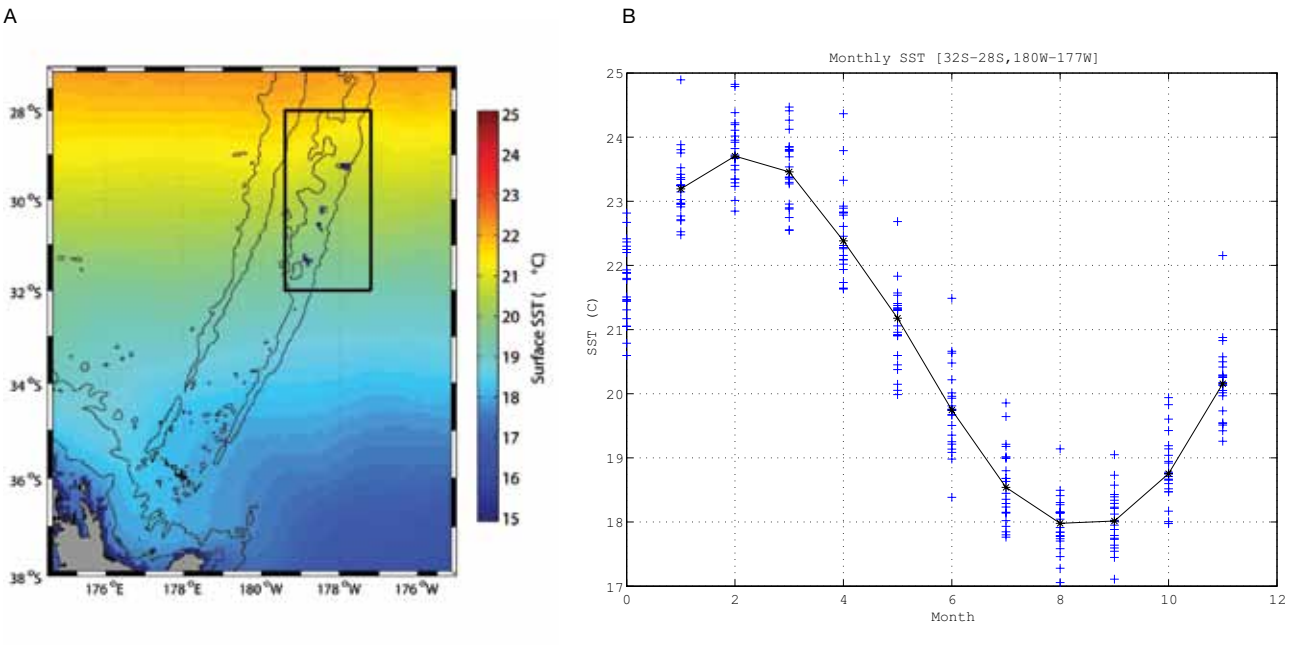

Figure 6. A. Mean sea-surface temperature for Kermadec Islands region from satellite AVHRR data for 1986–2007. Depths shallower than 500 m are masked. B. The annual cycle of SST from satellite AVHRR data.

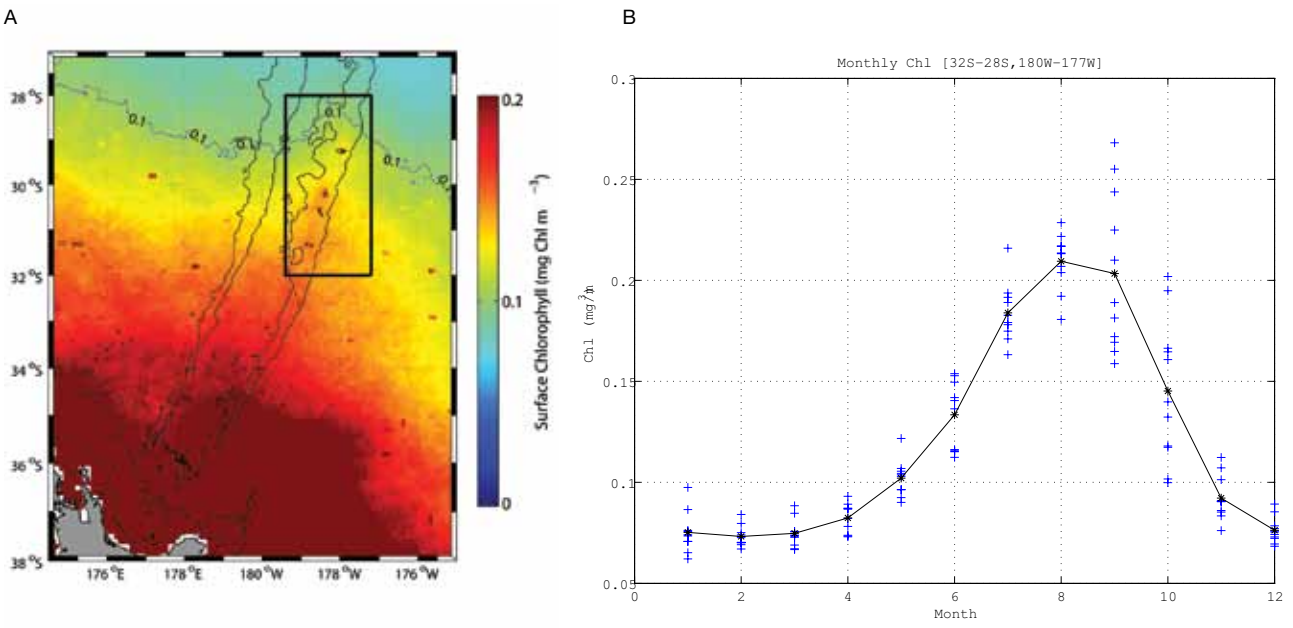

Figure 7. A. Mean chlorophyll from satellite SeaWifs data for 1997–2007. Depths shallower than 500 m are masked. B. The annual cycle of chlorophyll from satellite SeaWifs data.

The long-term mean significant wave height was in the range of 2.3 m to 2.5 m over the region, with directions from the south-southeast predominating. There is some seasonal variation in the wave climate. The summer months produce the lowest wave heights (c. 2.2 m) on average, with easterly waves predominating. The highest wave conditions on average occur in winter, particularly in June and July (c. 2.7 m), when the mean energy flux is from the south.

Bed orbital velocities are strongly dependent on water depth, becoming negligible in water more than a few wavelengths deep, which was the case for most of the region, except for a few grid cells in the vicinity of islands (for which values of 0.1–0.45 cm/s were calculated). Even for those places, it should be noted that the computed values are representative only for depths close to the average depth assumed in the simulations. Hence, the information on bed-orbital velocities from the present study is of limited value.

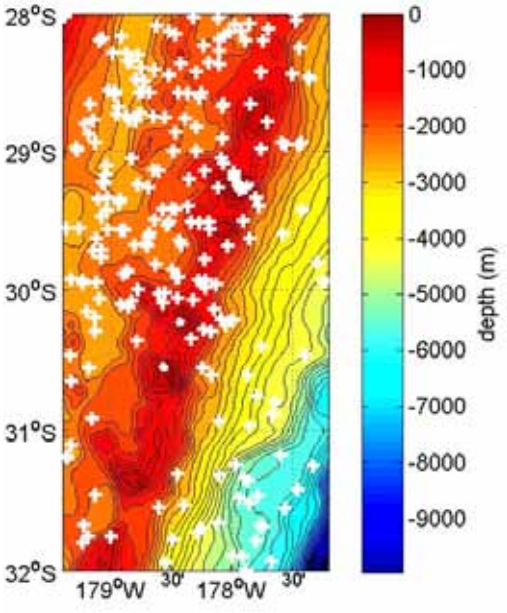

Figure 8. Positions of all Argo profiles collected 2002/03–2010 from the study region, overlaid on bathymetry.

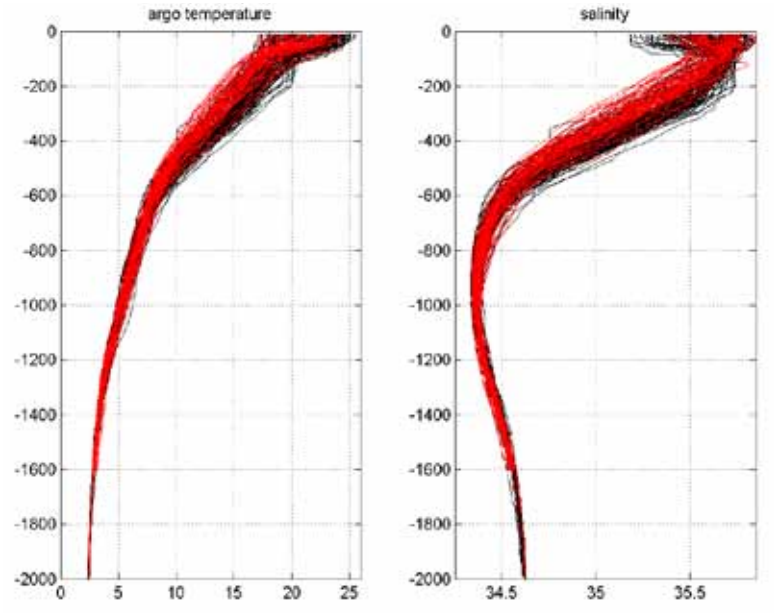

Figure 9. Temperature (left) and salinity (right) profiles collected from all of the Argo floats passing through the study region 2002/03–2010. The red profiles are from southeast of Kermadec Ridge; the black profiles are from northwest of the ridge.

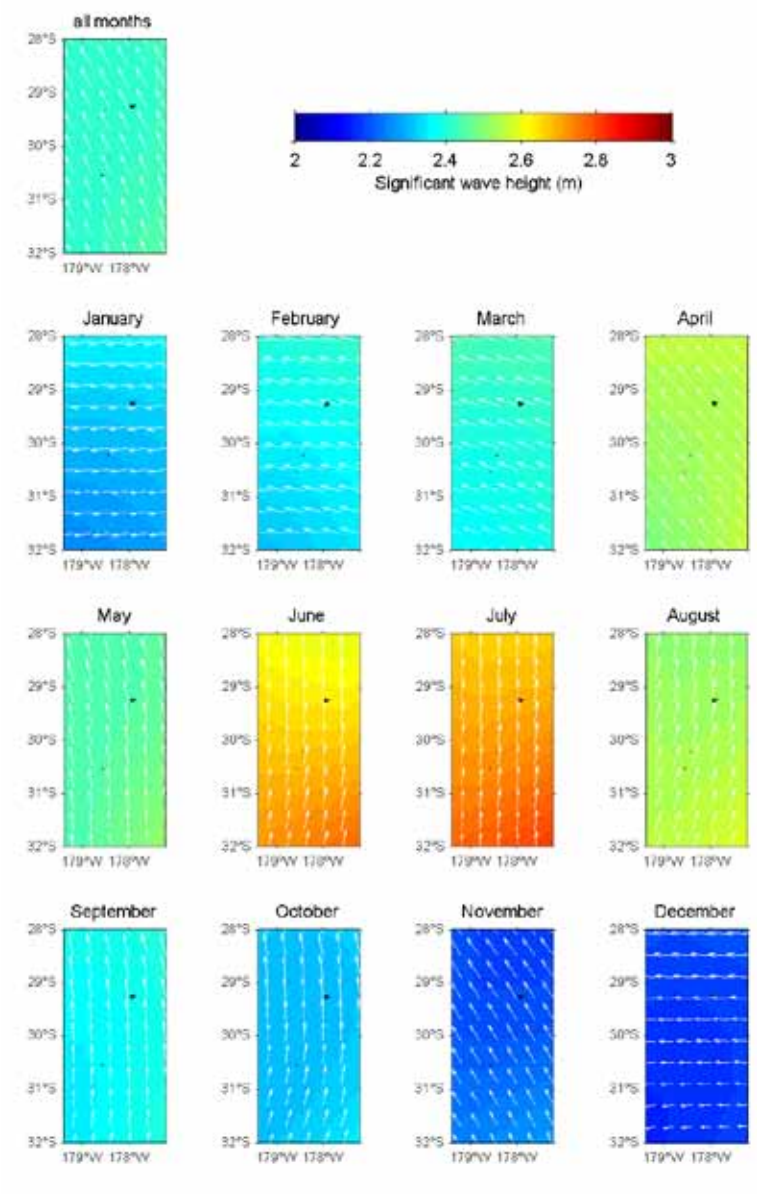

Figure 10. Significant wave height in the Kermadec region averaged over the NIWA-WAM hindcast period (February 1997 – March 2008). The arrows show the mean wave energy flux over the corresponding time, indicating the direction of net wave propagation. Results are shown for averages over the full period, and for each calendar month.

The annual cycle of monthly mean significant wave heights is evident in the time series data from the NOAA/NCEP Wavewatch III hindcast (Fig. 11). At the centre of the study region, the occurrence distribution of significant wave heights (Fig. 12) peaked near 2 m, and shows a long-term mean of 2.36 m, consistent with the results of the NIWA-WAM hindcast. There is, however, a long tail to the distribution, extending beyond 7 m, indicating the effects of occasional energetic storm systems in the region. Peak periods for that same site averaged 9.0 s (Fig. 13). Wave directions show a bimodal distribution (Fig. 14), with easterly conditions the most common, but also a strong contribution from southerly waves. There is very little wave energy from the northwest quadrant. We see from the wind rose (Fig. 15) that local winds were predominantly easterlies through to southeasterlies, but that winds from other directions are reasonably uniformly distributed (or, at least, distributed more uniformly than the wave directional distribution), emphasising that the southerly waves found in the region include a notable contribution from remotely-generated swell.

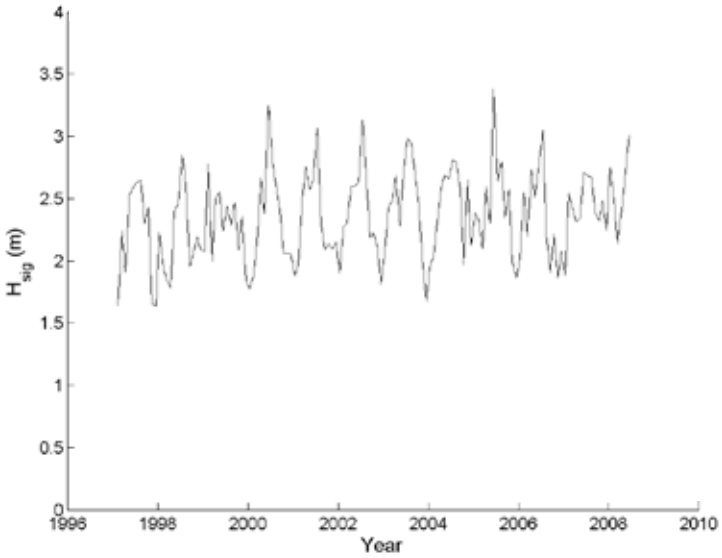

Figure 11. Time series of monthly mean significant wave heights (Hsig) for a site (178.75°W, 30°S) near the centre of the study region, using data from the NCEP Wavewatch III hindcast (February 1997 to June 2008).

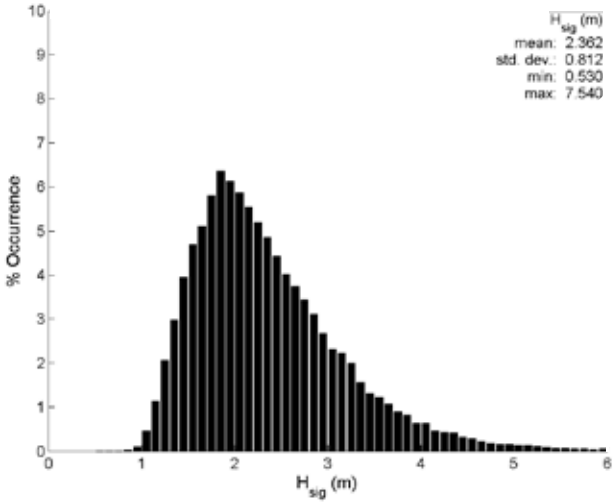

Figure 12. Occurrence distribution of significant wave height (Hsig) for a site (178.75°W, 30°S) near the centre of the Kermadec Islands region, using data from the NCEP Wavewatch III hindcast (February 1997 to June 2008).

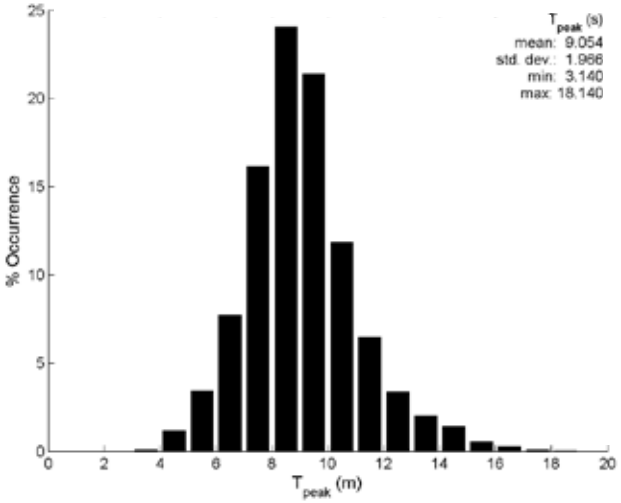

Figure 13. Occurrence distribution of peak wave period for a site (178.75°W, 30°S) near the centre of the Kermadec Islands region, using data from the NCEP Wavewatch III hindcast (February 1997 to June 2008).

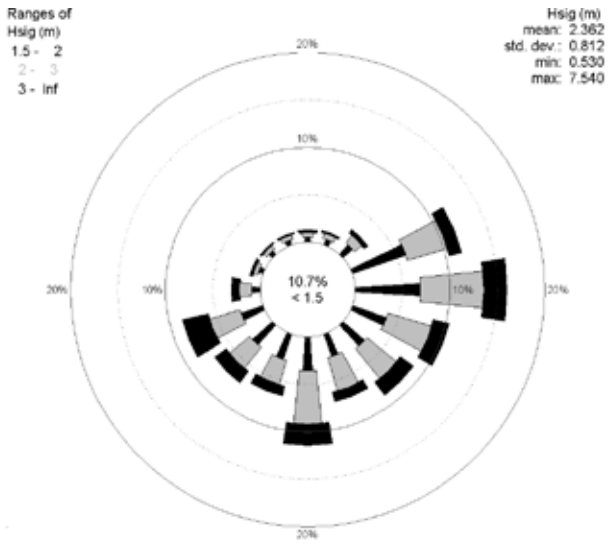

Figure 14. Wave rose (joint occurrence distribution of significant wave height and peak wave direction) for a site (178.75°W, 30°S) near the centre of the Kermadec Islands region, using data from the NCEP Wavewatch III hindcast (February 1997 to June 2008). Bars point towards the direction **from** which waves propagate.

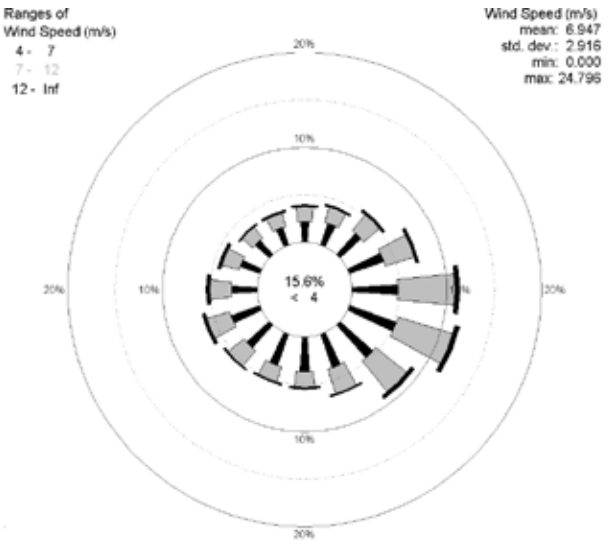

Figure 15. Wind rose (joint occurrence distribution of wind speed and direction) for a site (178.75°W, 30°S) near the centre of the Kermadec Islands region, using data from the NCEP Wavewatch III hindcast (February 1997 to June 2008). Bars point towards the direction **from** which waves propagate.

4. Discussion

The study region contains New Zealand's largest marine reserve. The Kermadec Marine Reserve was created in November 1990, extends 12 nautical miles out from the cliffs and boulder beaches of the various Kermadec Islands and rocks to the edge of the territorial sea, and covers 7450 km^2. In addition, all of the islands in the Kermadec group are part of a specially protected nature reserve. Being c. 1000 km northeast of New Zealand, this is the most remote conservation area managed by DOC. The pristine Kermadec Marine Reserve is the last remaining unfished area in New Zealand, and one of the few marine areas in the world where large predatory fishes are present in numbers and at sizes approaching that of natural, unfished populations.

The marine environment in the region is quite different from that of the New Zealand mainland because of its more subtropical location and isolation. Understanding the physical environment of the area is key to understanding the biology in the reserve, and knowledge of likely and possible connectivity is key to interpreting the local ecosystems.

4.1 Circulation and connectivity

The results of the connectivity studies are consistent with the mean flows in the study area being small and dominated by variability. Thus, virtually generated larvae dispersed in a roughly circular pattern from the chosen release locations, with a slight eastward bias introduced by the mean flow. In contrast, virtual releases from along the northeast coast of mainland New Zealand were largely contained within the East Auckland Current system and tended to track southward along the continental shelf. The connectivity studies indicate that the islands and seamounts within the study region are all relatively strongly interconnected, but that there is limited connection to mainland New Zealand. The modelling indicated that dispersion to neighbouring islands and seamounts would take 1–3 days, while dispersal between more distant islands in the Kermadec group would take up to 10 days. Dispersal to and from the northeast coast of mainland New Zealand would take between 20 and 50 days, depending on site location. Of course, dispersal

for real organisms will depend critically on their life cycles and environmental sensitivities. Thus, connectivity length scales could be much shorter than suggested by the virtual analysis (e.g. Wood & Gardner, 2007).

4.2 Productivity

Chlorophyll estimates from satellite (SeaWifs) measurements of ocean colour indicated that chlorophyll levels in the study area were largely typical of values for the larger, open ocean, subtropical gyre area (Murphy et al. 2001). The large-scale pattern is latitudinal, with cooler, more chlorophyll-rich water to the south, and warmer, chlorophyll-poorer waters to the north (Fig. 7a). There is a northward excursion over The Kermadec Ridge, with values at a given latitude on the ridge being equivalent to the higher values found 1–2° further south off the ridge. This is consistent with water masses following along constant potential vorticity contours (e.g. Gill 1982). That is, to conserve potential vorticity, water masses must move northward as they cross the Kermadec Ridge, thereby decreasing their planetary vorticity, and compensating for the decrease in water or pycnocline layer depth.

There is also a suggestion of higher values around the islands. These 'hotspots' must be interpreted with caution. While it is possible that there are real elevations in chlorophyll related to the islands (e.g. associated with island upwelling, tidal mixing, and increased productivity in the coastal band), it is also possible that they are a result of increased sediment loading in the waters near the islands being misinterpreted as chlorophyll by the algorithms used to extract chlorophyll from ocean colour. In situ measurements are necessary to resolve this ambiguity. The mean values for chlorophyll along the Kermadec Ridge of about 0.1 mg/m3 are typical for this latitude in the subtropics, and lower than typically found around New Zealand (usually < 0.3 mg/m3), and much lower than the very high values 0.5 mg/m3) found over the Chatham Rise (Murphy et al. 2001). In addition, chlorophyll variability along the Kermadec Ridge is very small compared with variations found elsewhere in New Zealand's Exclusive Economic Zone (Murphy et al. 2001).

4.3 Water column characteristics

There are no in situ nutrient measurements available from the study area, but nutrient levels are likely to be low, based on the area being in the oligotrophic subtropical gyre and the generally low chlorophyll concentrations.

The vertical properties of temperature and salinity are all consistent with the location of the study area in the centre of the subtropical gyre. The only remarkable feature of the vertical structure is that there was quite high variability well down into the main thermocline. This variability is even more notable given that there were only weak mean flows in the area. The cause of the variability in the temperature and salinity profiles is likely to be strong internal tides, generated by the interaction of surface tides with the Kermadec Ridge and other ridges and seamounts in the area. There was a systematic change in the water properties between the southeastern and northwestern sides of the Kermadec Ridge, with the profiles from the southeast indicating cooler and fresher water at given depths compared with areas northwest of the ridge.

4.4 Wave climate

The long-term mean significant wave height was in the range of 2.3 m to 2.5 m over the whole region, with waves predominantly from the south-southeast. There was some seasonal variation evident in the wave climate. The summer months produced the lowest wave heights (c. 2.2 m) on average, with a predominance of easterly waves. The highest wave conditions on average occurred in winter, particularly in June and July (c. 2.7 m), when the mean energy flux is from the south.

In the wider New Zealand region, weather systems in the Southern Ocean, with a predominance of strong westerlies, produce energetic wave conditions throughout the year, but particularly in winter. Swell from these systems propagates into lower latitudes, mostly from the southwest. In the Kermadec region, the New Zealand landmass provides some shelter from southwesterly swell, but southerly swell can reach this region. The result is that the study area has a wave climate that is slightly atypical by New Zealand standards. More locally, weather systems in the Pacific Ocean and Tasman Sea produce less energetic waves on average in the Kermadec region, but the larger of these events can result in high waves at any time of year.

The calculation of bed orbital velocities needs highly accurate bathymetry, which means results from the present study are of limited value. To improve our knowledge, further work is required using higher-resolution bathymetric data in the vicinity of the islands, where depths are shallow enough for wave motion to have significant penetration to the bed.

4.5 Possible effects of climate change on currents, waves and stratification

The location of the study region near the middle of the subtropical gyre and away from ocean fronts and boundary currents would suggest that changes in the Kermadec region due to climate change are likely to be progressive rather than involving a regime shift.

The predicted climate changes around New Zealand include warming, sea level rise and about a 10% increase in the mean westerly wind component over the next 50 years (Mullan et al. 2001). These changes, however, should not greatly impact circulation around the Kermadec Islands. The variability in the currents should continue to dominate the mean flow, and the region is likely to be north of the latitudes where zonal wind changes are predicted (Mullan et al. 2001).

There are likely to be changes in ocean stratification in the region, though, with the warming temperatures resulting in increased stratification. It is also possible that the stratification will increase and winter mixed layer depths increase as a result of the subtropical gyre 'spinning up'. A study of the South Pacific subtropical gyre spinning up through the 1990s (Roemmich et al. 2007) postulated that increasing westerlies at high latitudes caused changes in gyre circulation. If, in a warming world, the high-latitude westerlies indeed increase, gyre spin up could become stronger or permanent, and this spin up would result in a deeper, warmer pool of water in the gyre centre—including around the study region. The main ramification of increased stratification is likely to be decreased productivity—as the ocean becomes more strongly layered, it becomes harder to mix nutrients up from depth to supply the euphotic zone.

The effects of potential future global climate change on wave conditions in the New Zealand region remain uncertain. Wave climate is influenced by both locally-generated waves, and distantly-generated swell. The above-mentioned prediction of a c. 10% increase in the westerly wind component over the next 50 years (Mullan et al. 2001) is likely to reduce the easterly component of the Kermadecs' locally-generated wave energy flux. Because the predicted increase in westerly winds occurs in latitudes south of New Zealand, an increase in the contribution of the southerly swell component of the wave climate in the Kermadec region could be expected. At a wider scale, the incidence, and particularly the intensity, of tropical cyclones and other storms is expected to change. This can also have a significant effect on wave climate, notably on the intensity of extreme events. However, the present state of climate science means that the likely changes in storm occurrence throughout the Pacific are ill-defined, and thorough studies simulating New Zealand wave conditions, by forcing wave models with input winds derived from appropriate atmospheric climate models, are yet to be carried out.

5. Conclusions

The Kermadec Islands study region has relatively subtle oceanography. Situated towards the centre of the South Pacific subtropical gyre, the region has a weak mean circulation which is dominated by variability. At depth in the Kermadec Trench, the strong, globally-significant Deep Western Boundary Current dominates, but it has little or no effect on the shallow ocean above it. The importance of small length- and time-scale variability in currents and environmental parameters (e.g. temperature, salinity) together with complicated local bathymetry mean that available data poorly resolve the system. In particular, there is effectively no sub-surface nutrient, chlorophyll or plankton information. Our understanding of the system would be enhanced by collecting more *in situ* environmental data; expanding our knowledge of the bathymetry and incorporating that knowledge into wave models; examining the outputs of steadily-improving numerical models as they become available; and developing regional models.

6. Acknowledgements

This study was funded by DOC (Investigation Number 4071).

7. References

Chiswell, S.M.; Moore, M.I. 1999: Internal tides near the Kermadec Ridge. *Journal of Physical Oceanography* 29: 1019–1035.

Chiswell, S.M.; Rickard, G.J.; Bowen, M.M. 2007: Eulerian and Lagrangian eddy statistics of the Tasman Sea and southwest Pacific Ocean, *Journal of Geophysical Research-Oceans 112*, C10004, doi:10.1029/2007JC004110.

Chiswell, S.M.; Rickard, G.J. 2008: Eulerian and Lagrangian statistics in the Bluelink numerical model and AVISO altimetry: validation of model eddy kinetics. *Journal of Geophysical Research 113*: C10024, doi:10010.11029/12007JC004673.

Gill, A.E. 1982: Atmosphere-ocean dynamics. Academic Press. 662 p.

Gorman, R.M. 2005: Numerical wave forecasting for the New Zealand region. Pp. 179–184 in Townsend, M.; Walker, D. (Eds): Coasts and ports, coastal living – living coast. Proceedings of the Australasian Conference, 20–23 September 2005, Adelaide, South Australia. Institute of Engineers, Adelaide.

Lavelle, J.W.; Massoth, G.J.; Baker, E.T.; de Ronde C.E.J. 2008: Ocean current and temperature time series at Brothers volcano. *Journal of Geophysical Research 113*: C09018, doi: 10.1029/2007JC004713.

Moore, M.I.; Wilkin, J.L. 1998: Variability in the South Pacific Deep Western Boundary Current from current meter observations and a high-resolution global model, *Journal of Geophysical Research 103(C3)*: 5439–5457, doi:10.1029/97JC03207.

Mullan, B.; Bowen, M.; Chiswell, S. 2001: The crystal ball: model predictions of future climate. *Water and Atmosphere 9*: 10–11.

Murphy, R.J.; Pinkerton, M.H.; Richardson, K.M.; Bradford-Grieve, J.M.; Boyd, P.W. 2001: Phytoplankton distributions around New Zealand derived from SeaWiFS remotely-sensed ocean colour data. *New Zealand Journal of Marine and Freshwater Research 35*: 343–362.

Olson, D.B. 2007: Lagrangian biophysical dynamics. Pp. 275–348 in Griffa, A.; Kirwin, A.D.; Mariano, A.J.; Ozgokmen, T.M.; Rossby, R. (Eds): Lagrangian analysis and prediction of coastal and ocean dynamics. Cambridge University Press, Cambridge.

Reynolds, R.W.; Smith, T.M. 1994: Improved global sea surface temperature analyses. *Journal of Climate 7*: 929–948.

Roemmich, D.; Gilson, J.; Davis, R.; Sutton, P.; Wijffels, S.; Riser, S. 2007: Decadal spin-up of the South Pacific Subtropical Gyre. *Journal of Physical Oceanography 37*: 162–173.

Sharples, J.; Moore, E.M.; Abraham, E.R. 2001: Internal tide dissipation, mixing, and vertical nitrate flux at the shelf edge on NE New Zealand. *Journal of Geophysical Research 106*: 14 069–14 081.

Smith, W.H.F.; Sandwell, D.T. 1997: Global sea floor topography from satellite altimetry and ship depth soundings. *Science 277*: 1956–1962.

Stevens, C.L.; Abraham, E.R.; Moore, C.M.; Boyd, P.W.; Sharples, J. 2005: Observations of small-scale processes associated with the internal tide encountering an island. *Journal of Physical Oceanography 35*: 1553–1567.

Sutton, P.J.H.; Roemmich, D. 2001: Ocean temperature climate off north-east New Zealand. *New Zealand Journal of Marine and Freshwater Research 35*: 553–565.

Tolman, H.L. 1999: User manual and system documentation of WAVEWATCH-III Version 1.18, NOAA / NWS / NCEP / OMB. *Technical Note 166*, 110 p. (http://polar.ncep.noaa.gov/mmab/papers/tn166/OMB_166.pdf)

Tolman, H.L.; Balasubramaniyan, M.; Burroughs, L.D.; Chalikov, D.V.; Chao, Y.Y.; Chen, H.S.; Gerald, V.M. 2002: Development and implementation of wind-generated ocean surface wave models at NCEP. *Weather and Forecasting 17(2)*: 311–333.

Warren, B.A.; Whitworth, T.; Moore, M.I.; Nowlin, W.D. 1994: Slight northwestward inflow to the deep South Fiji Basin. *Deep-Sea Research I 41(5/6)*: 953–956.

Whitworth, T.; Warren, B.A.; Nowlin, W.D.; Rutz, S.B.; Pillsbury, R.D.; Moore, M.I. 1999: On the deep western boundary current in the Southwest Pacific Basin. *Progress in Oceanography 43(1)*: 1–54.

Wood, A.B.; Gardner, J.P.A. 2007: Small spatial scale population genetic structure in two limpet species endemic to the Kermadec Islands, New Zealand. *Marine Ecology Progress Series 349*: 159–170.